Electronic Supplementary Material (ESI) for ChemComm.


**Supporting Information**

# Reversible Stimuli-Responsive Chromism of a Cyclometallated Platinum(II) Complex

Qingshu Zheng,[a,b] Stefan Borsley,[a] Tao Tu[b] and Scott L. Cockroft[a]*

[a] EaStCHEM School of Chemistry, University of Edinburgh, Joseph Black Building, David Brewster Road, Edinburgh EH9 3FJ, UK.

[b] Shanghai Key Laboratory of Molecular Catalysis and Innovative Materials, Department of Chemistry, Fudan University, 2005 Songhu Road, Shanghai 200438, China.

# Contents

# S1. General experimental procedures

Unless stated otherwise, all chemicals were purchased from commercial sources (Sigma Aldrich UK, Acros UK, VWR UK or Fluorochem UK) and used without further purification. Dry solvents were obtained by means of a "Glass Contour" brand solvent purification system, where solvents were passed through filter columns and dispensed under an argon atmosphere. Flash column chromatography was performed using Geduran® Si60 (40-63 mm, Merck, Germany) as the stationary phase, and thin-layer chromatography (TLC) was performed on pre-coated silica gel plates (0.25 mm thick, 60F254, Merck, Germany) and observed under UV light ($l_{max}$ 254 nm). Mass spectrometry was performed using a Bruker MicrOTOF II or Bruker MicrOTOF11 spectrometer for ESI-HRMS. $^{1}$H and $^{13}$C NMR spectra were recorded on Bruker Ultrashield 400 MHz, Bruker Ascend 500 MHz equipped with a DCH cryoprobe, and Bruker AVANCE III HD at a constant temperature of 25 °C, unless otherwise stated. $^{1}$H, $^{13}$C, and $^{195}$Pt chemical shifts are reported in parts per million (ppm) from low to high field. $^{1}$H and $^{13}$C values are referenced to the literature values for chemical shifts of residual non-deuterated solvent, with respect to tetramethylsilane. $^{195}$Pt is referenced externally to $K_2PtCl_6$ at 0 ppm. Diffusion ordered spectroscopy (DOSY), Nuclear overhauser effect spectroscopy (NOESY) and Exchange spectroscopy (EXSY) were recorded on Bruker AVANCE III HD 500 MHz. Standard abbreviations indicating multiplicity are used as follows: bs (broad singlet), d (doublet), dd (doublet of doublets), m (multiplet), q (quartet), s (singlet), t (triplet), tt (triplet of triplets), *J* (coupling constant). All spectra were analysed using MestReNova software. NMR tubes, precision glassware and glass syringes were dried under vacuum before use. Fluorescence spectra were recorded by using a Shimadzu RF-5300PC spectrophotometer. UV-vis spectroscopy was performed on a Varian Cary 50 Scan UV Visible Spectrophotometer. Non-deuterated anhydrous solvents were used directly as commercially obtained anhydrous solvents, or were redistilled under reduced pressure from analytical-grade solvents.

Complexes **1**-Pt and **1**-Pd were synthesised as previously described. All structural and characterisation data matched literature values.[S1]

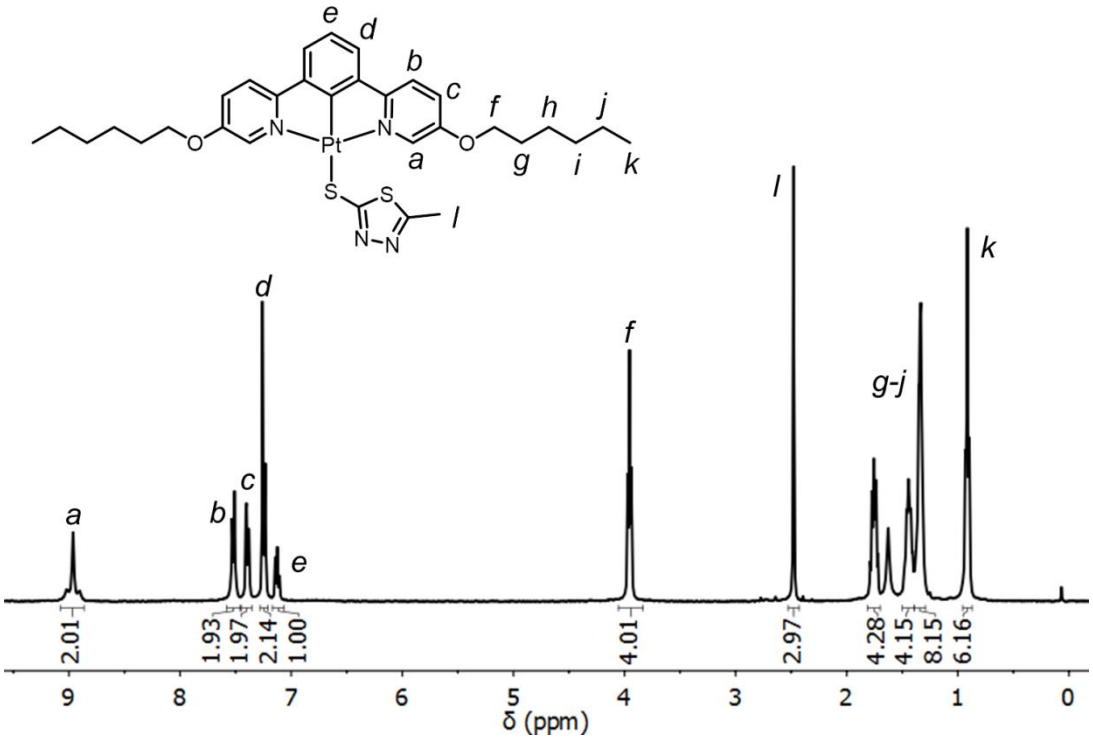


**Figure S1** $^{1}$H NMR spectrum of complex **1**-Pt in $CDCl_3$.

# S2. Solid State Characterisation

## S2.1 Visual characterisation

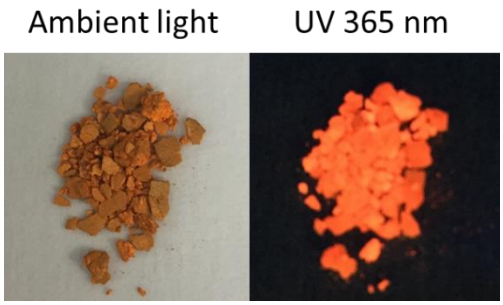


**Figure S2** Photographs of the complex **1**-Pt under ambient light and under UV light (365 nm).

## S2.2 Solid State Emission Spectroscopy

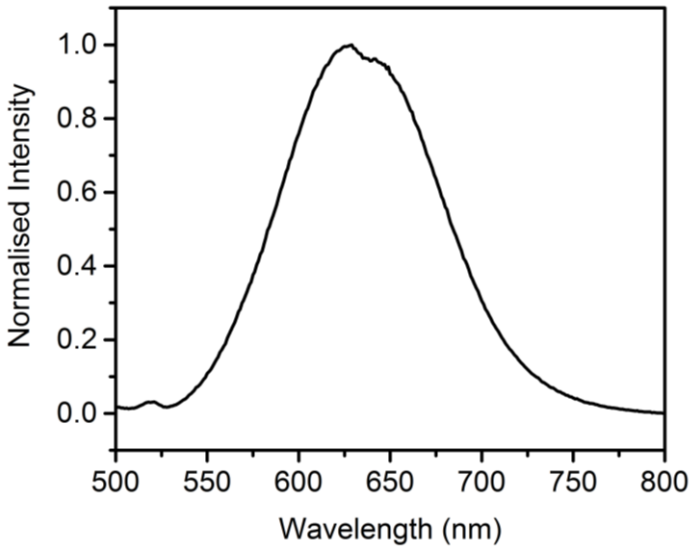


**Figure S3** Solid-state emission spectrum of complex **1**-Pt excited at 480 nm.

## S2.3 Crystallography

Crystal structures of complexes **1**-Pt and **1**-Pd were previously published.[S1]

# S3. Solution-Phase Behaviour

## S3.1 $^1$H NMR dilution experiments

$^1$H NMR dilution experiments of complexes **1**-Pt or **1**-Pd in $CDCl_3$ were previously published.[S1]

$^1$H NMR dilution experiments of complexes **1**-Pt in $CD_3OD$ was performed via following procedures:

Stock solutions of complex **1**-Pt was dissolved in the $CD_3OD$ at high concentrations. A known volume of the stock solution was added to a Wilmad screw-cap NMR tube containing 350 μL of solvent. $^1$H NMR spectra were recorded. Further amounts of the stock solution were added and spectra were obtained. The procedure was repeated at several different concentrations.

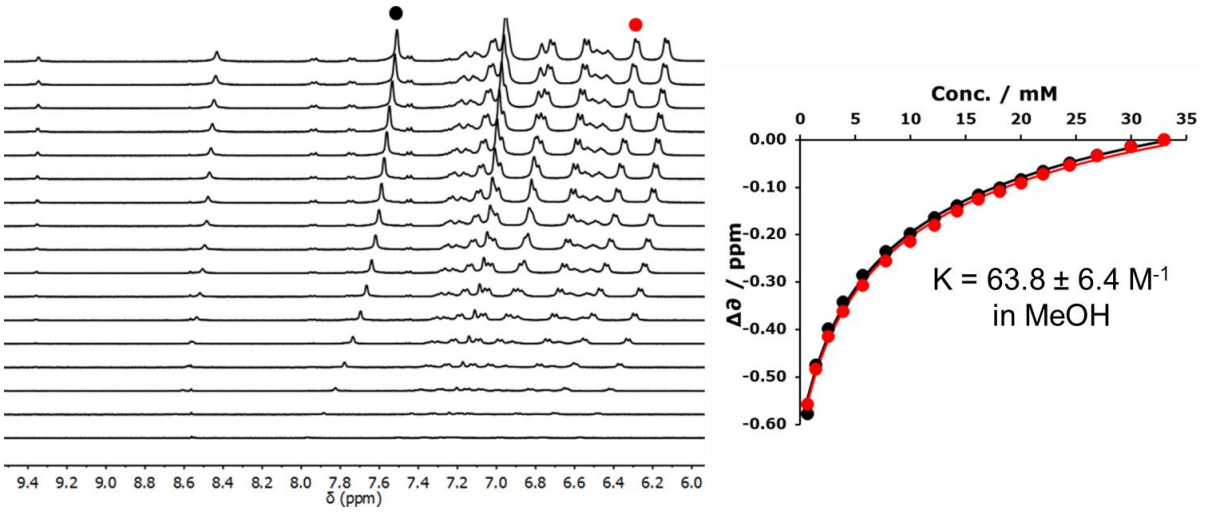


**Figure S4** Partial $^1$H NMR spectra of dilution experiments (500 MHz, $CD_3OD$, 298 K) for complex **1**-Pt and binding isotherms generated based on peaks around 7.7 ppm (black dot) and 6.4 ppm (red dot). The data is fitted to a 1:1 binding isotherm (solid line).

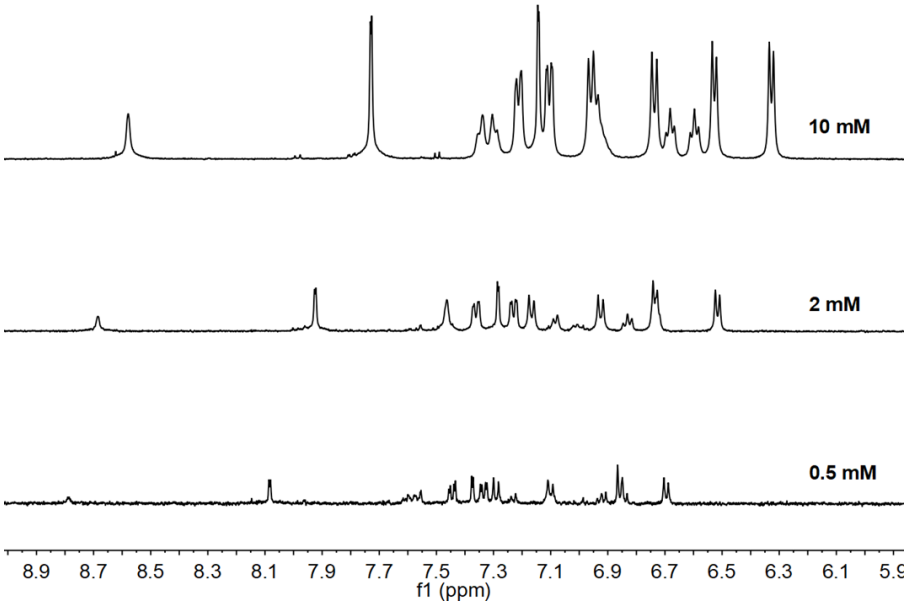


**Figure S5** Partial $^{1}$H NMR spectra (500 MHz, $CD_3OD$, 298 K) of complex **1**-Pt at different concentrations.

## S3.2 UV-vis dilution experiments

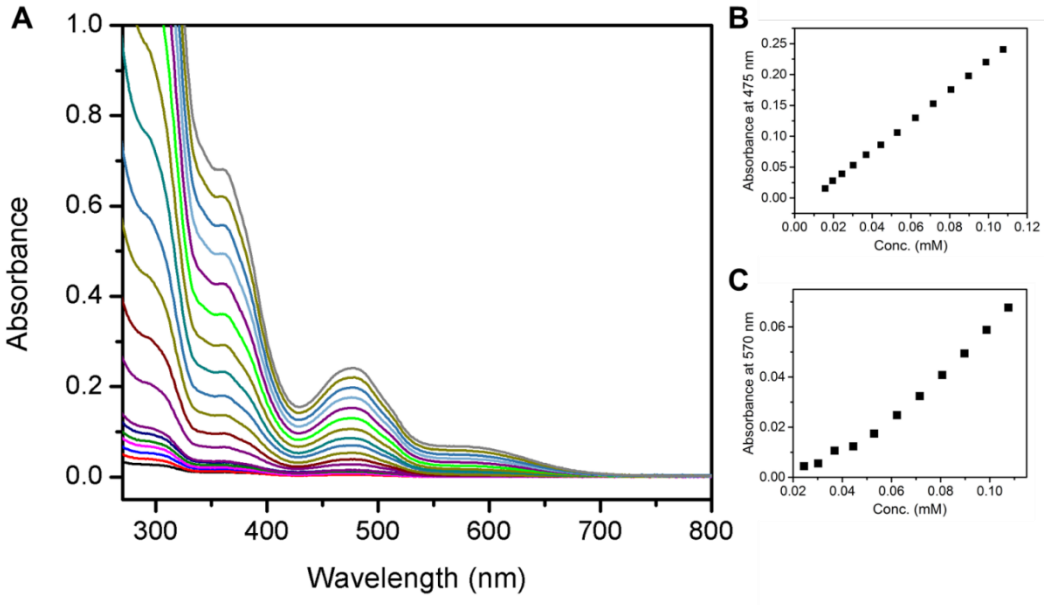


**Figure S6** (**A**) UV-vis absorption spectra of dilution experiments (MeOH, 298 K) for complex **1**-Pt. (**B**) Linear response in absorption at 475 nm. (**C**) Non-linear response in absorption at 570 nm.

## S3.3 Time dependant NMR spectroscopy

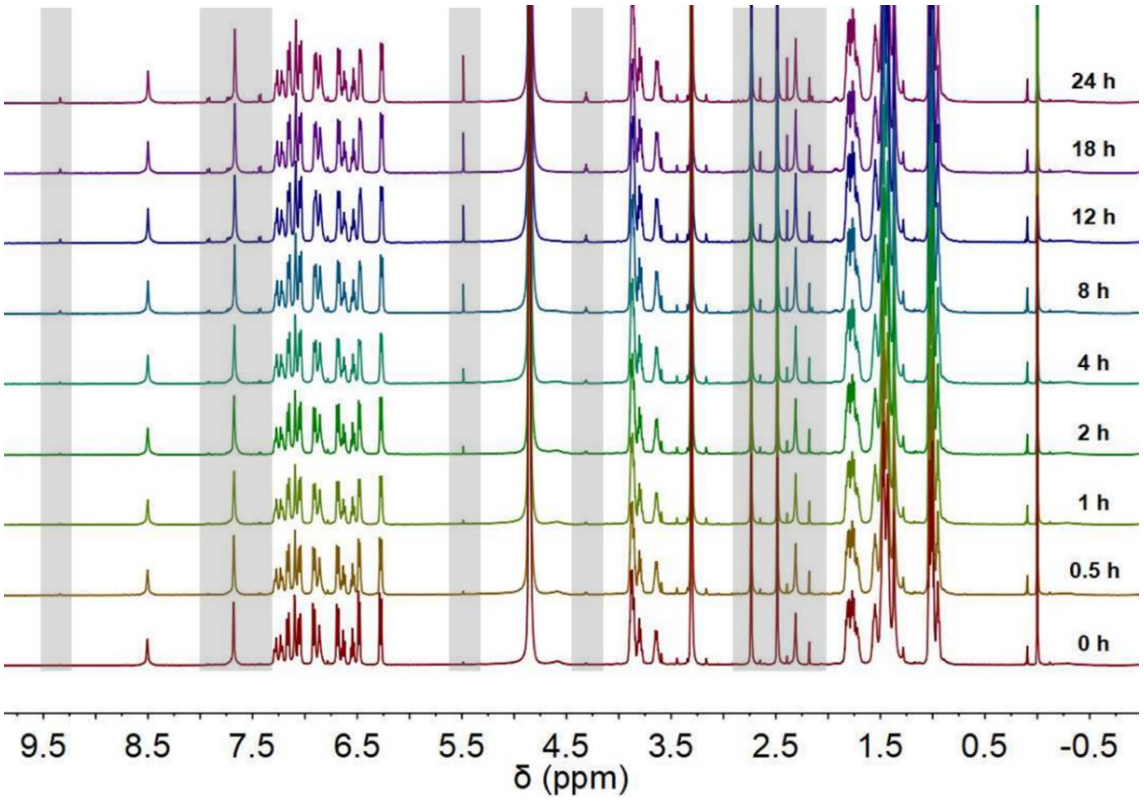


**Figure S7** Partial $^{1}$H NMR spectra (500 MHz, $CD_3OD$, 298 K) of complex **1**-Pt over time. Regions with new resonances emerging over time are highlighted in grey.

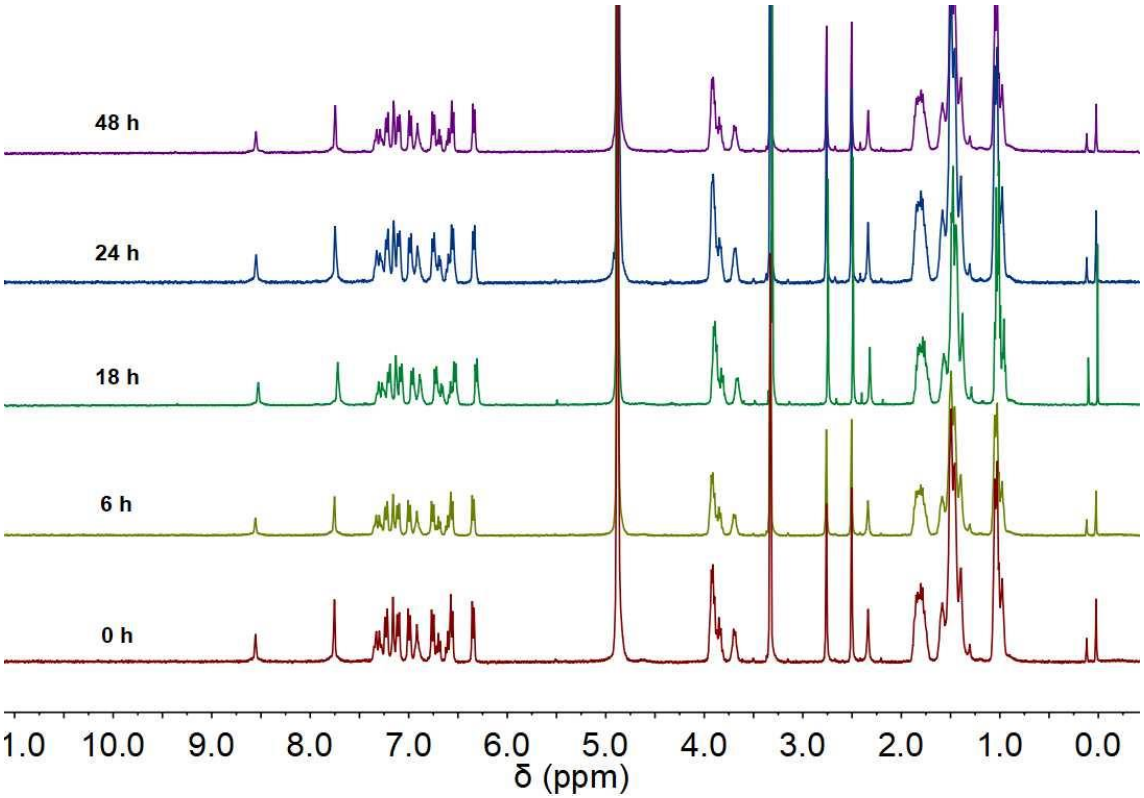


**Figure S8** $^{1}$H NMR spectra (500 MHz, 298 K) of complex **1**-Pt over time in degassed methanol-$d_4$.

## S3.4 Images of complex 1-Pt over time

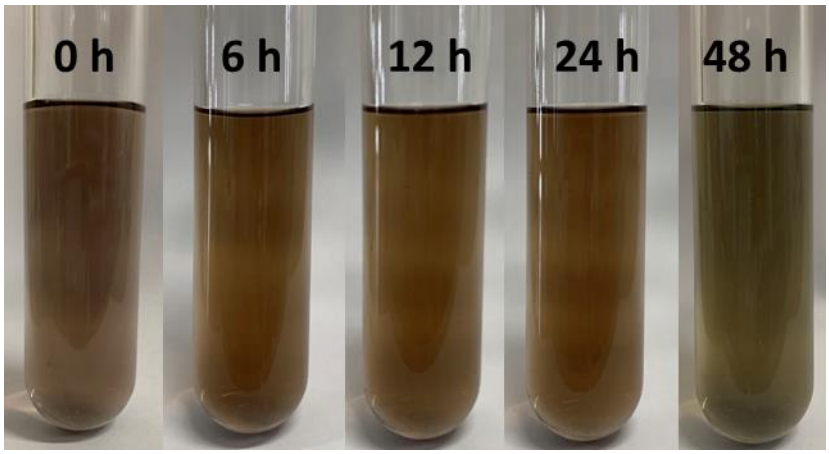


**Figure S9** Images of complex 1-Pt in degassed anhydrous methanol in a Schlenk tube after standing for different period of time.

## S3.5 Time dependant UV-vis spectroscopy

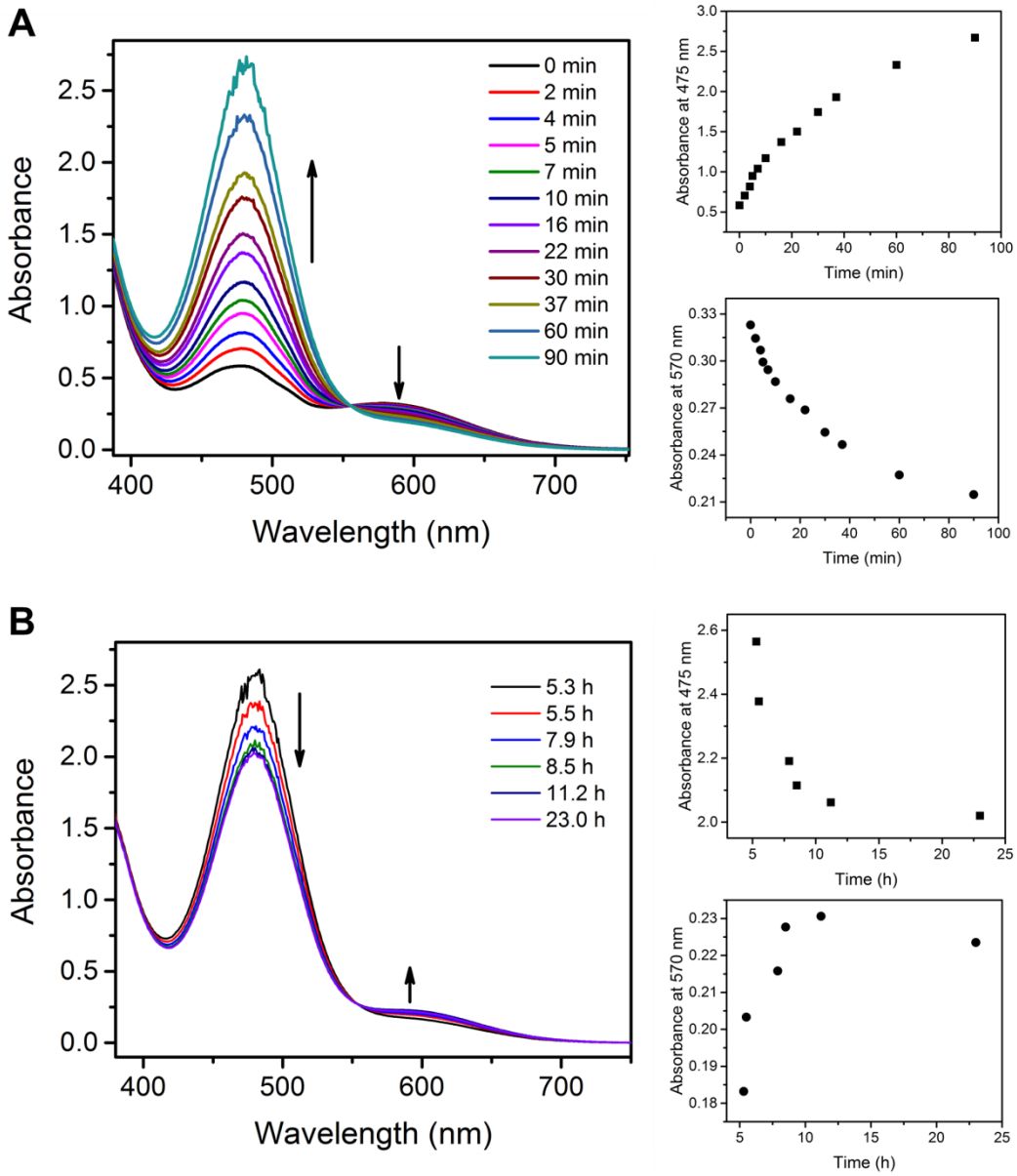


**Figure S10** UV-vis spectra of **1**-Pt (0.25 mM) showing the changing absorbance over time for (**A**) the first 90 mins after adding solvent and (**B**) 5–24 hours after adding solvent. The change in absorbance at 475 nm and 570 nm is shown on the small graphs to the right.

## S3.6 Variable temperature UV-vis spectroscopy

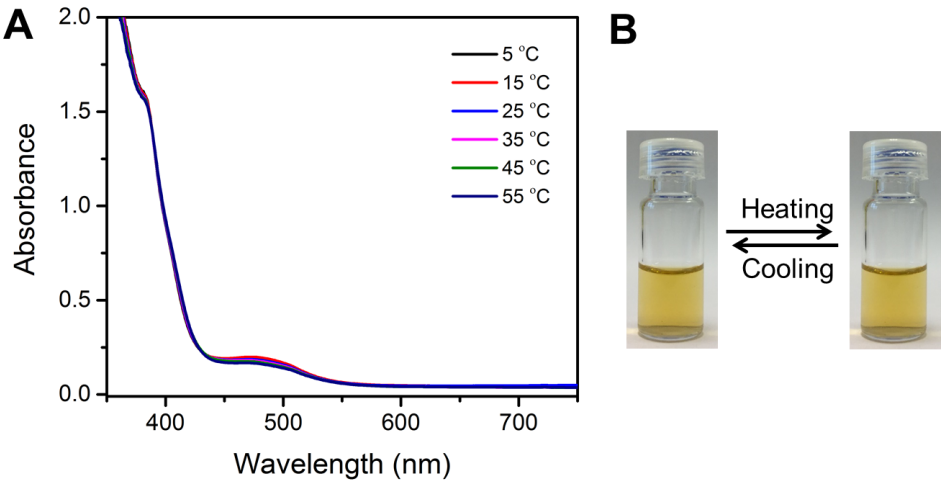


**Figure S11** (**A**) Temperature-dependant UV-vis spectra of complex **1**-Pt in $CHCl_3$ (0.2 mM) 24 hours after preparation. (**B**) Photographs of complex **1**-Pt in $CHCl_3$ 24 hours after preparation under ambient light showing no thermochromic response.

## S3.7 Solution-Phase Emission Spectroscopy

Solutions of **1**-Pt in polar solvents ([**1**-Pt] = 0.05 mM) showed strong emission at ~620 nm (480 nm excitation) (Figure S12, ESI†), which are red-shifted compared to the two emission peaks at 520 nm and 550 nm observed in apolar solvents, indicating the presence of different species in polar solvents. Further increasing the concentration of **1**-Pt in polar solvents (Figures S13–S14, ESI†) allows the appearance of new broad peaks at 650–750 nm, corresponding to metal-metal-to-ligand charge transfer (MMLCT).

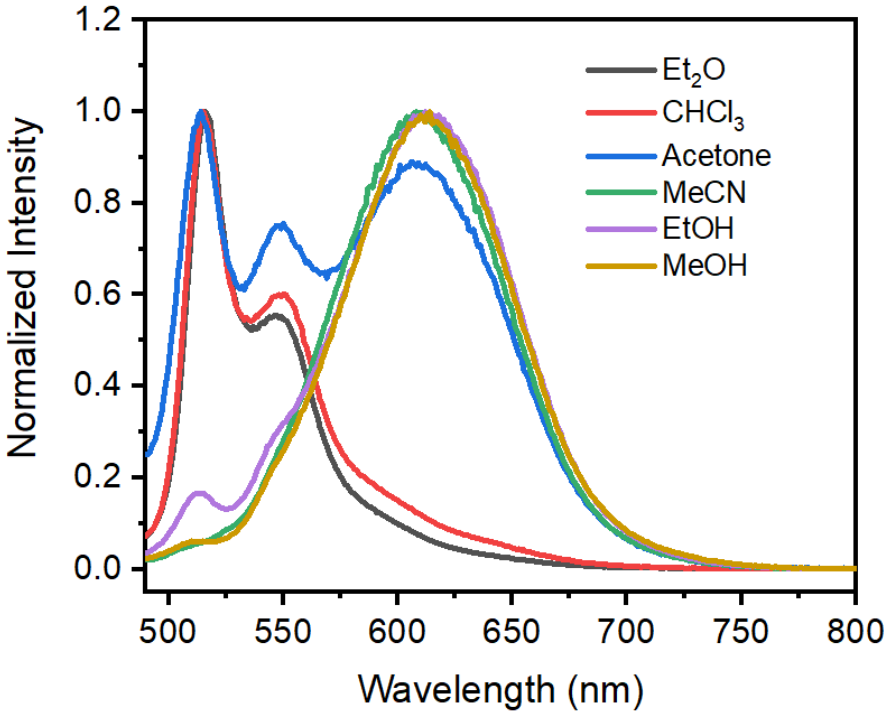


**Figure S12** Emission spectrum of complex **1**-Pt in different solvents ($5 \times 10^{-5}$ M) excited at 470 nm.

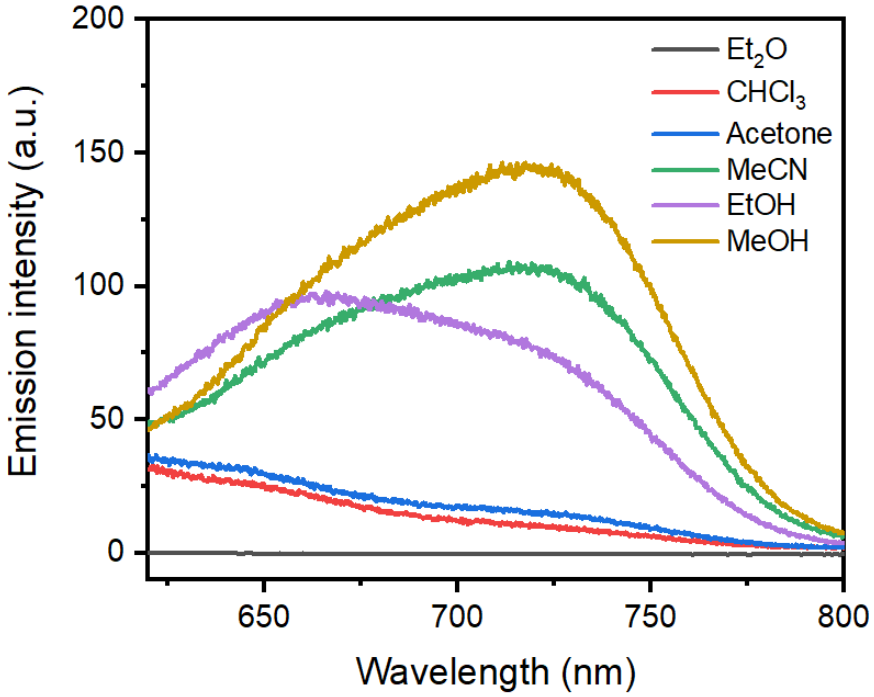


**Figure S13** Emission spectrum of complex **1**-Pt in different solvents ($5 \times 10^{-4}$ M) excited at 570 nm. Broad peaks corresponding to MMLCT were observed in polar solvents (MeOH, EtOH, acetonitrile) but not in less polar or apolar solvents ($Et_2O$, $CHCl_3$, acetone), suggesting **1**-Pt tended to aggregate in polar solvents.

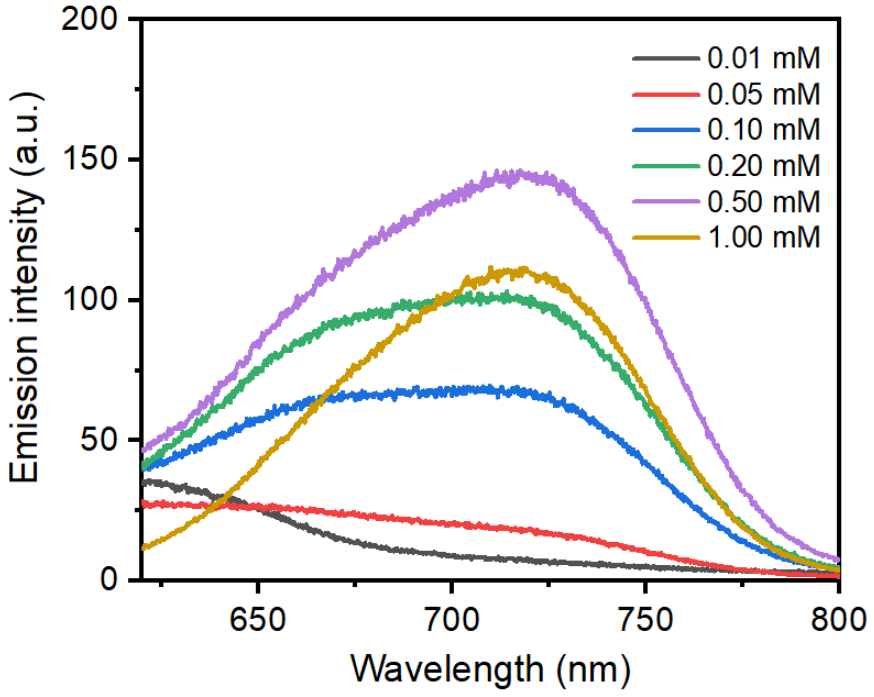


**Figure S14** Concentration-dependent fluorescence emission spectrum of complex **1**-Pt in methanol excited at 570 nm. The intensity of the broad peaks corresponding to MMLCT increased upon increasing the concentration of **1**-Pt from $1 \times 10^{-5}$ mM to $5 \times 10^{-4}$ mM. But further increase of concentration to $10^{-3}$ mM would slightly quench the fluorescence.

# S4. Further characterisation of complex 1-Pt in MeOH

## S4.1 $^{1}$H and $^{195}$Pt NMR spectroscopy

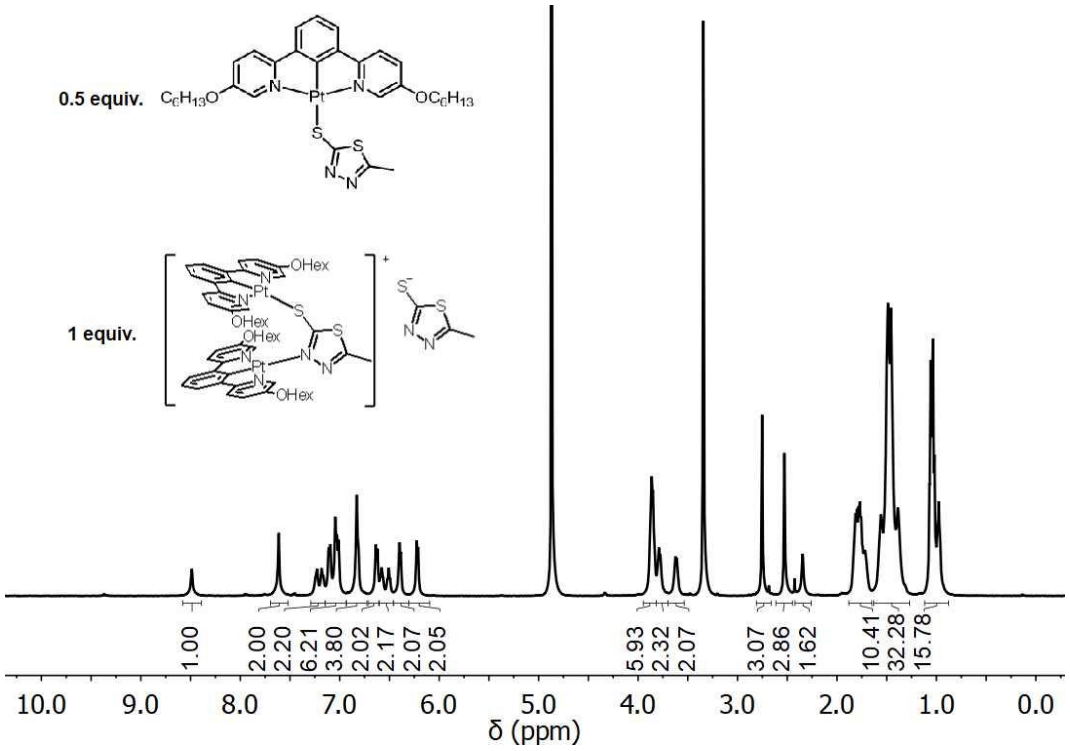


**Figure S15** $^{1}$H NMR spectrum of complex **1**-Pt in $CD_3OD$ measured immediately after dissolution. The solution appear to have rapidly equilibrated to form a 1:2 mixture of **1**-Pt to $[2\text{-}Pt_2]^+$ complex.

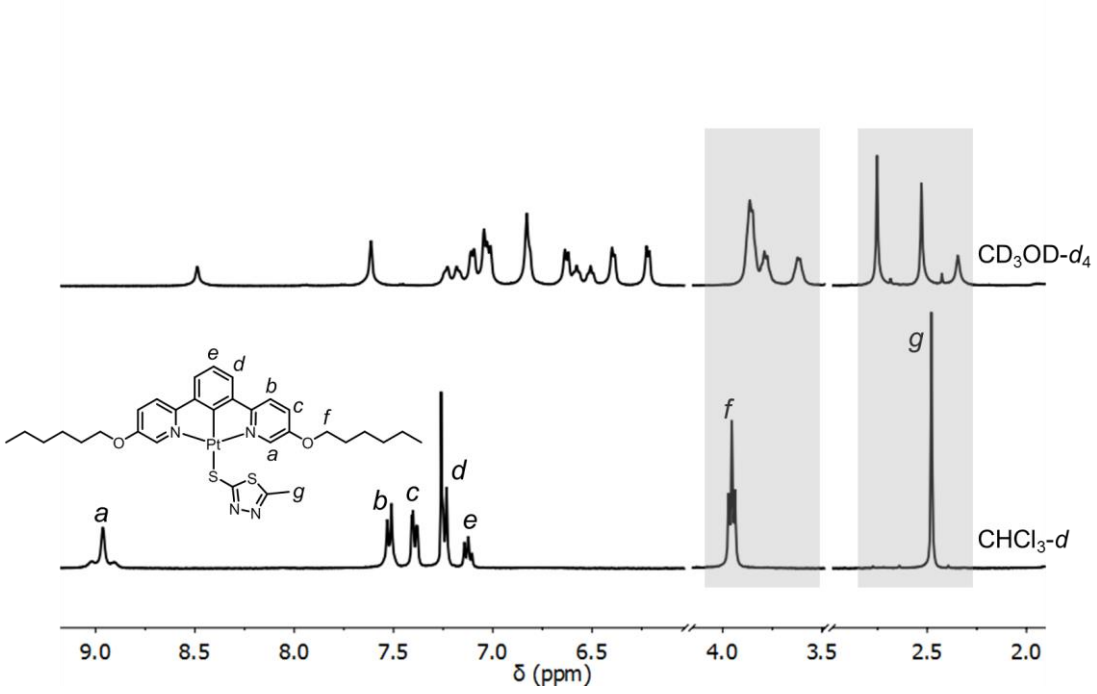


**Figure S16** Comparison of the partial $^{1}$H NMR spectra (500 MHz, 298 K) of complex **1**-Pt in $CDCl_3$ (bottom) and $CD_3OD$ (top). The single peaks in $CDCl_3$ split into 3 distinct signals in $CD_3OD$.

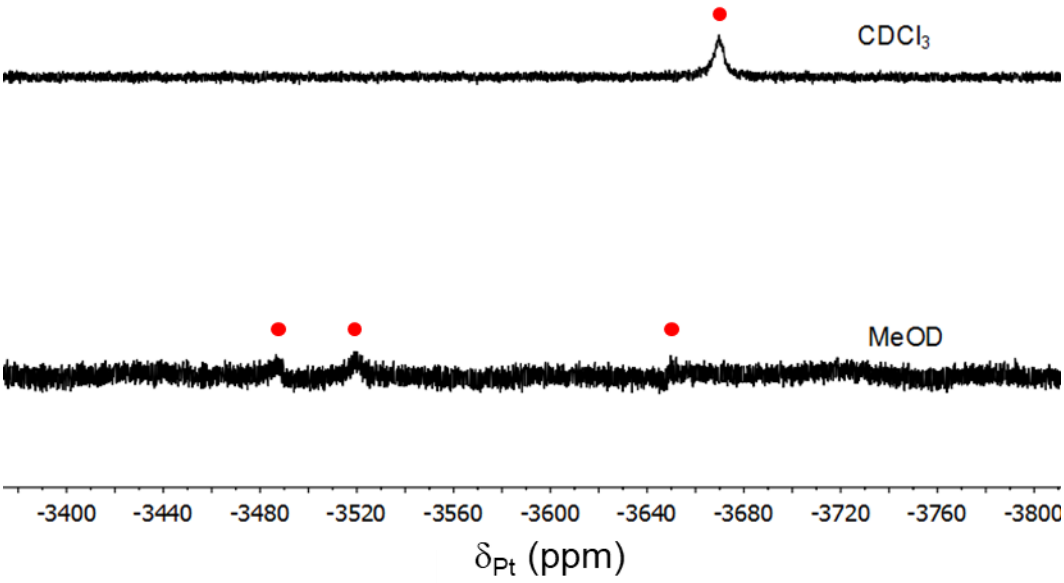


**Figure S17** Partial $^{195}$Pt NMR spectra (500 MHz, 298 K) of complex **1**-Pt in $CDCl_3$ (top) and $CD_3OD$ (bottom). Despite the inherent broadness, the single peak in $CDCl_3$ is seen to split into 3 distinct signals in $CD_3OD$.

## S4.2 Synthesis and characterisation of possible cationic diPt complex.

**Scheme S1** Synthesis of cationic diPt complex.

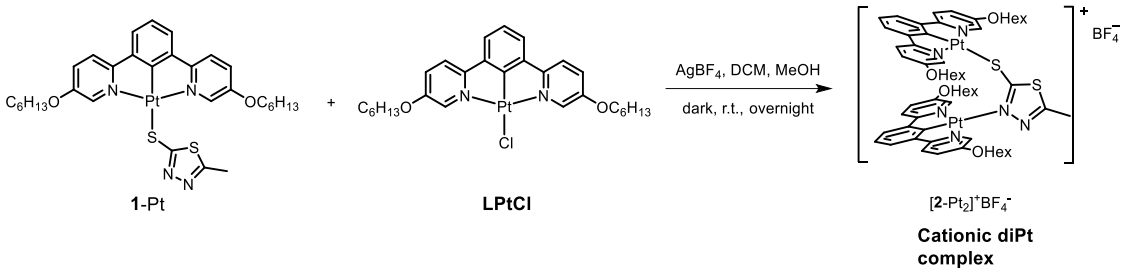


The cationic diPt complex [**2**-$Pt_2$]$^+BF_4^-$ was synthesised according to a modified procedure of literature.[S2] Complex **1**-Pt (0.15 mmol, 0.099 g), complex **LPtCl** (0.15 mmol, 0.113 g) were dissolved in $CH_2Cl_2$ (40 mL) in a round bottom flask wrapped with foil, yielding solution 1. Another flask wrapped with foil was charged $AgBF_4$ (0.18 mmol, 0.035 g) and MeOH (15 mL), giving solution 2. The obtained solution 2 was added dropwise into solution 1 at room temperature. Precipitate was generate immediately and the mixture changed to blue quickly. The mixture was stirred overnight at r.t. After filtration, the filtrate was concentrated. The raw powder was collected and purified by column chromatography ($CH_2Cl_2$:MeOH = 15:1). The dark blue powder was collected and dried under vacuum (60% yield). $^1$H NMR (400 MHz, $CDCl_3$) δ 7.90 (d, *J* = 2.7 Hz, 2H), 7.23 (dd, *J* = 8.9, 2.8 Hz, 2H), 7.20 – 7.12 (m, 4H), 7.07 (d, *J* = 8.9 Hz, 2H), 6.91 (d, *J* = 8.9 Hz, 2H), 6.76 (dd, *J* = 8.2, 7.0 Hz, 1H), 6.68 – 6.60 (m, 3H), 6.46 (d, *J* = 7.6 Hz, 2H), 3.98 – 3.69 (m, 8H), 2.70 (s, 3H), 1.74 (m, 8H), 1.54 – 1.27 (m, 24H), 1.02 – 0.85 (m, 12H). $^{13}$C NMR (101 MHz, $CDCl_3$) δ 163.12, 159.83, 159.37, 154.15, 154.06, 140.08, 139.34, 138.35, 138.04, 124.29, 123.77, 123.47, 123.32, 122.44, 122.20, 120.46, 120.32, 69.12, 69.02, 31.88, 31.75, 29.41, 29.15, 25.86, 25.67, 22.81, 22.73, 16.29, 14.26, 14.21.

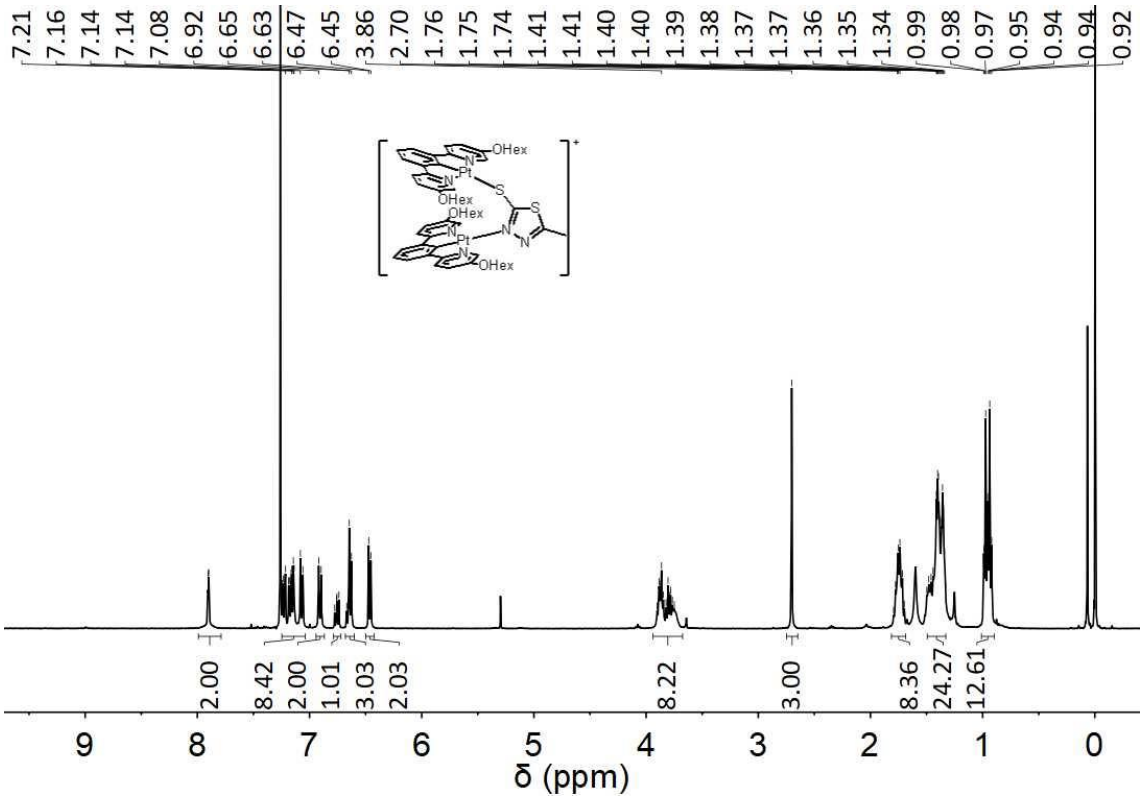


**Figure S18** $^1$H NMR spectra (500 MHz, 298 K) of cationic diPt complex [**2**-$Pt_2$]$^+BF_4^-$ in $CDCl_3$.

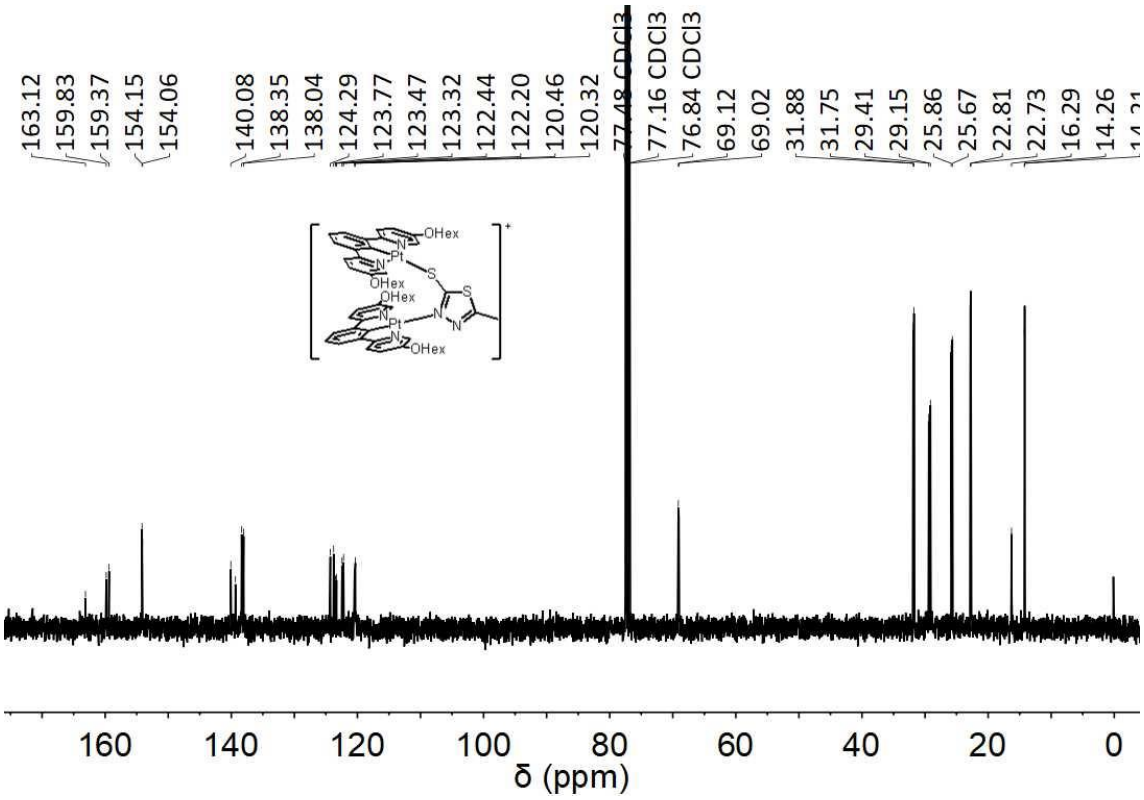


**Figure S19** $^{13}C$ NMR spectra (500 MHz, 298 K) of the cationic diPt complex [**2**-$Pt_2$]$^+BF_4^-$ in $CDCl_3$.

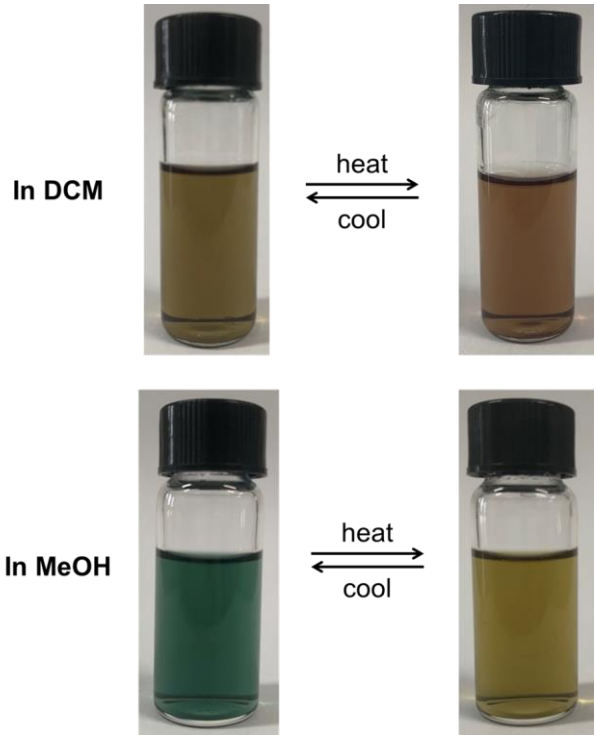


**Figure S20** Images of the cationic diPt complex [**2**-$Pt_2$]$^+BF_4^-$ in $CH_2Cl_2$ (DCM) and methanol upon heating and cooling. These solvatochromic and thermochromic properties are consistent with those of **1**-Pt, again suggesting the presence of the cationic [**2**-$Pt_2$]$^+$ complex in the solution of **1**-Pt in methanol.

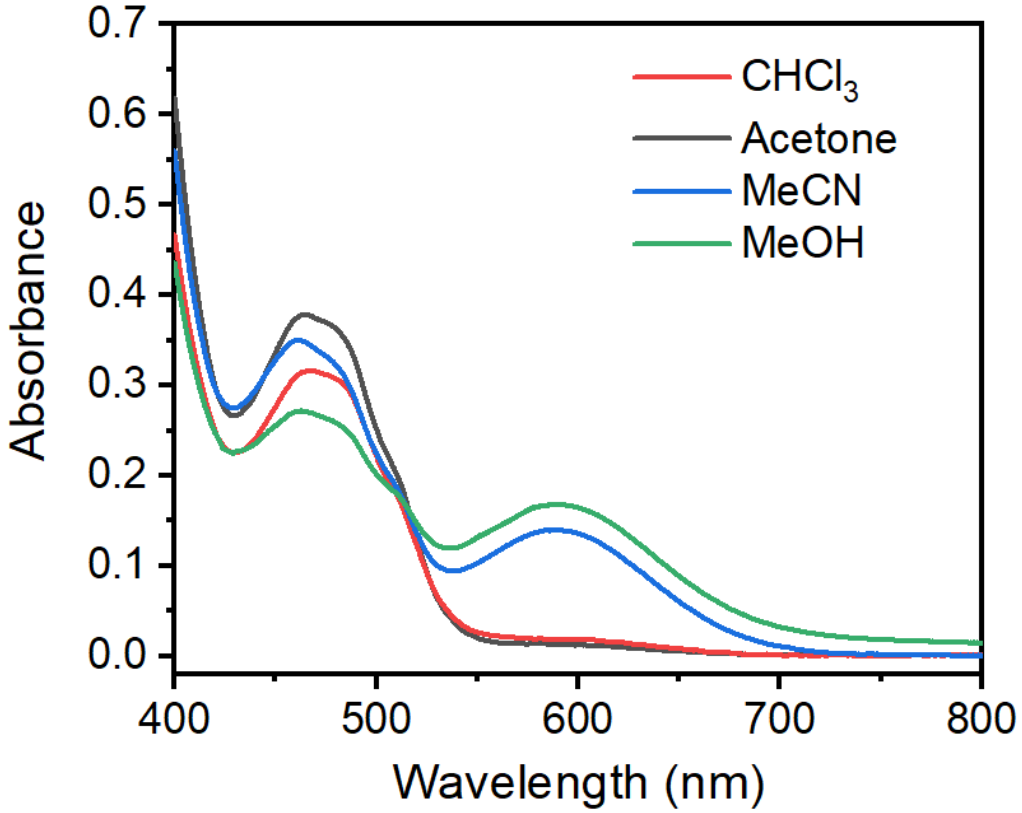


**Figure S21** UV-Vis spectra of the complex [**2**-$Pt_2$] $BF_4$ (0.1 mM) in different solvents at room temperature.

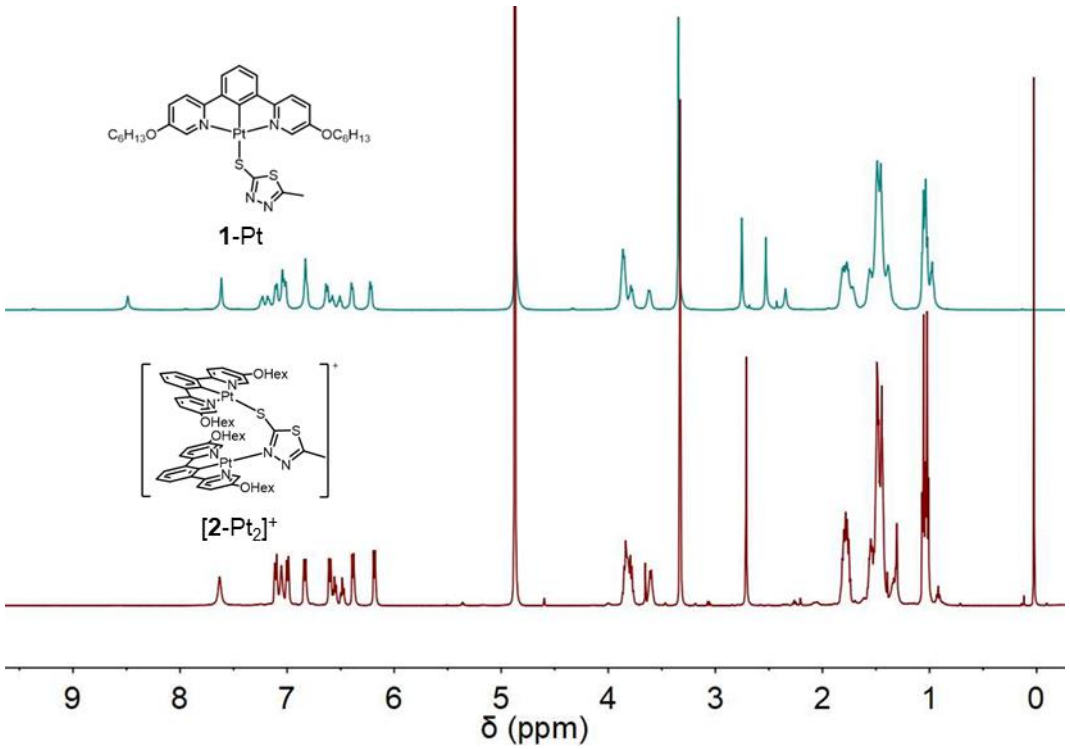


**Figure S22** $^1H$ NMR spectra (500 MHz, 298 K) of complex **1**-Pt and the cationic [**2**-$Pt_2$]$^+$ complex in $CD_3OD$.

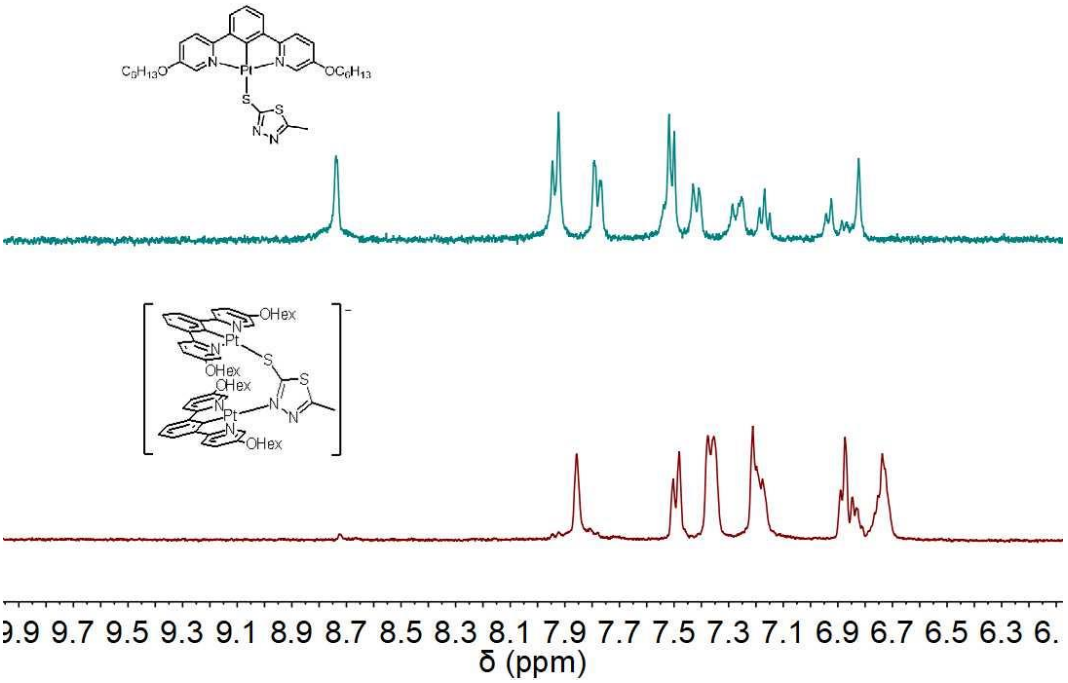


**Figure S23** $^{1}$H NMR spectra (500 MHz, 298 K) of complex **1**-Pt and the cationic [**2**-$Pt_2$]$^{+}$ complex in DMSO-$d_6$.

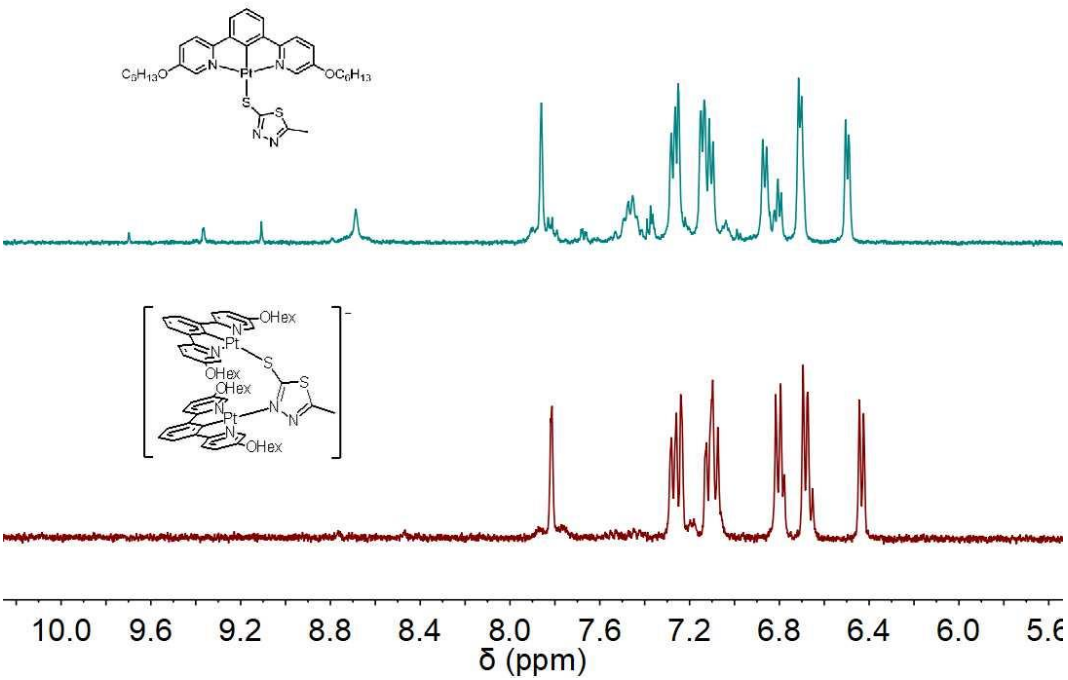


**Figure S24** $^{1}$H NMR spectra (500 MHz, 298 K) of complex **1**-Pt and the cationic [**2**-$Pt_2$]$^{+}$ complex in acetonitrile-$d_3$.

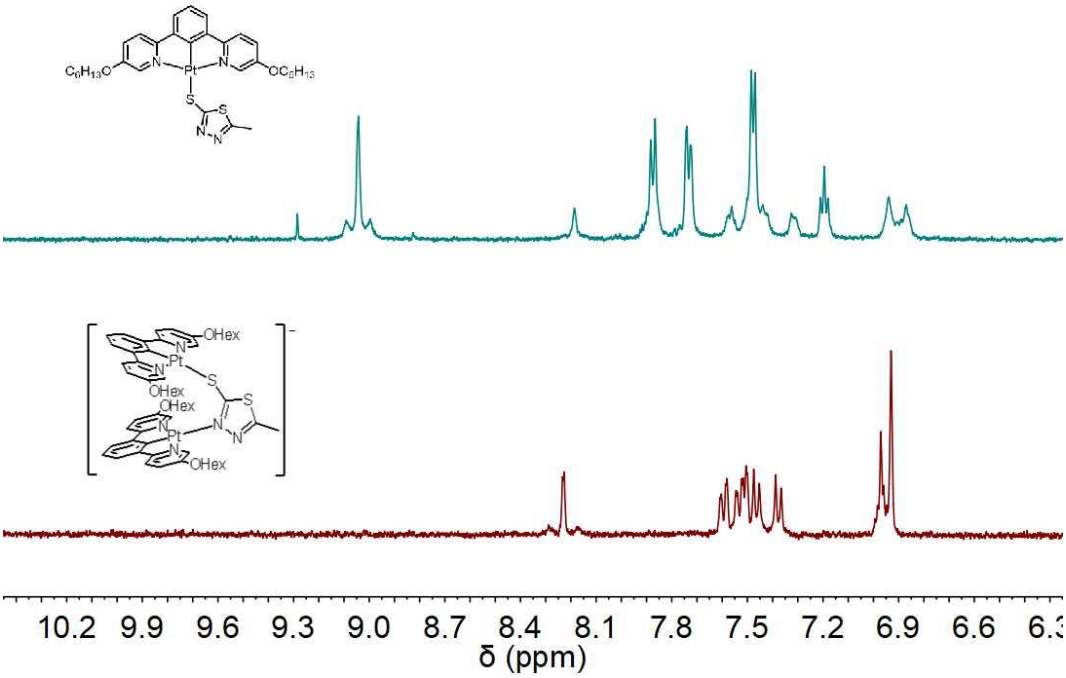


**Figure S25** $^{1}$H NMR spectra (500 MHz, 298 K) of complex **1**-Pt and the cationic [**2**-$Pt_2$]$^{+}$ complex in acetone-$d_6$.

## S4.3 2D NMR spectroscopy

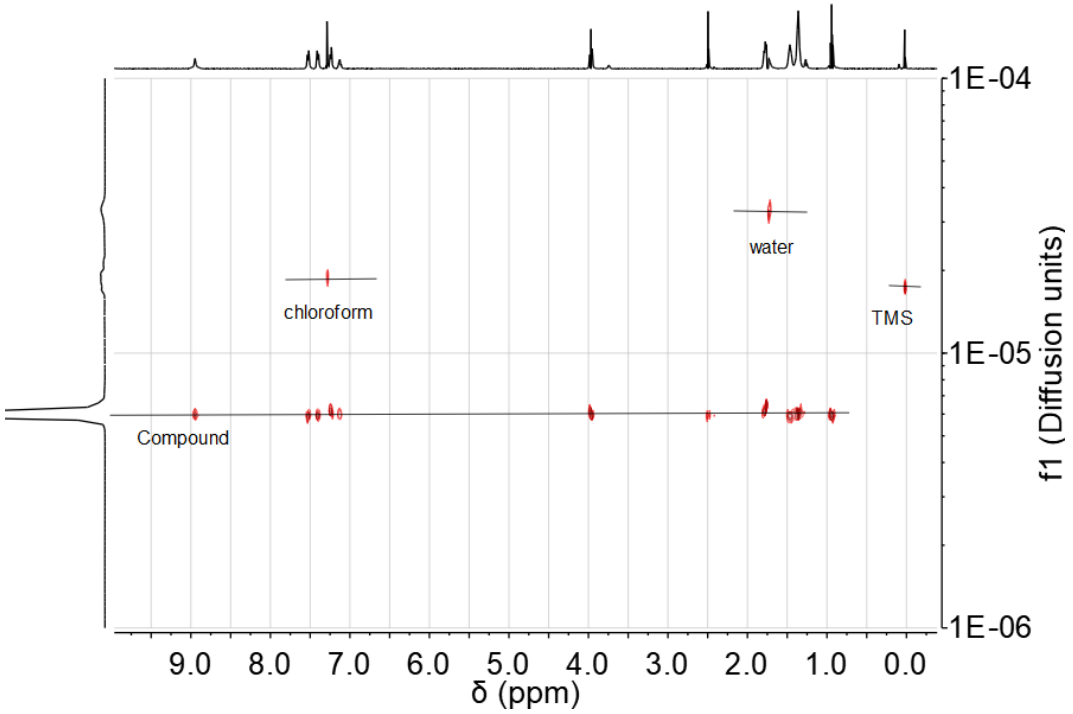


**Figure S26** DOSY spectra (500 MHz, 298 K) of complex **1**-Pt in chloroform-*d*.

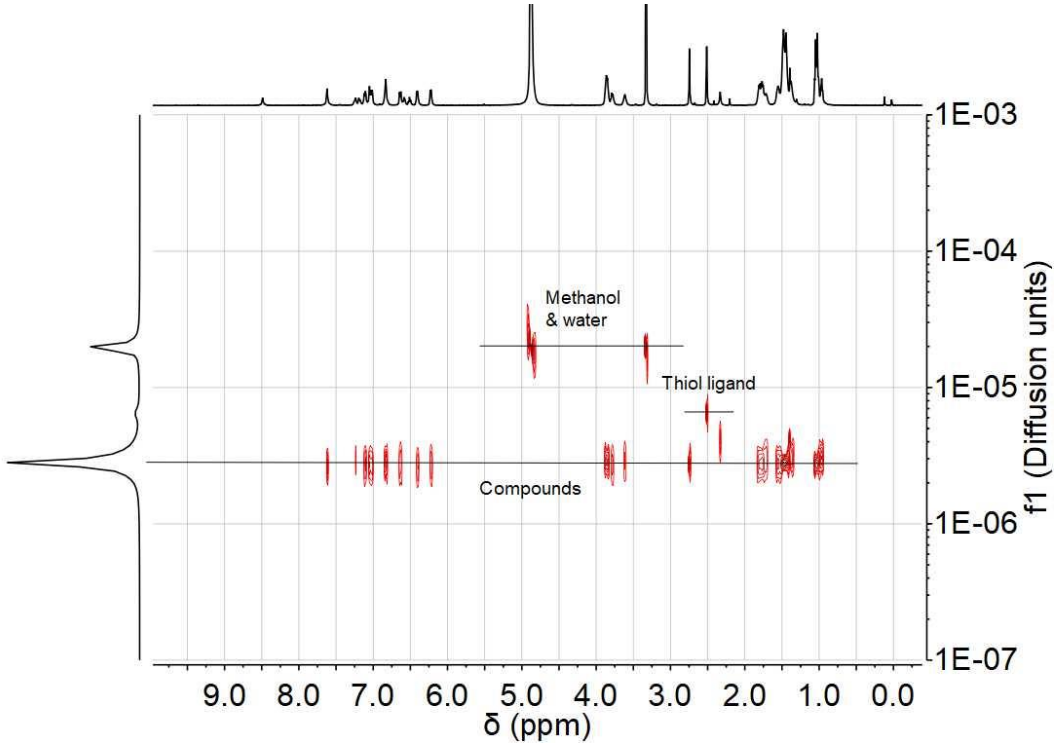


**Figure S27** DOSY spectra (500 MHz, 298 K) of complex **1**-Pt in $CD_3OD$. The broad signal of compounds and the presence of free thiol ligand suggest the presence of cationic diPt complexes.

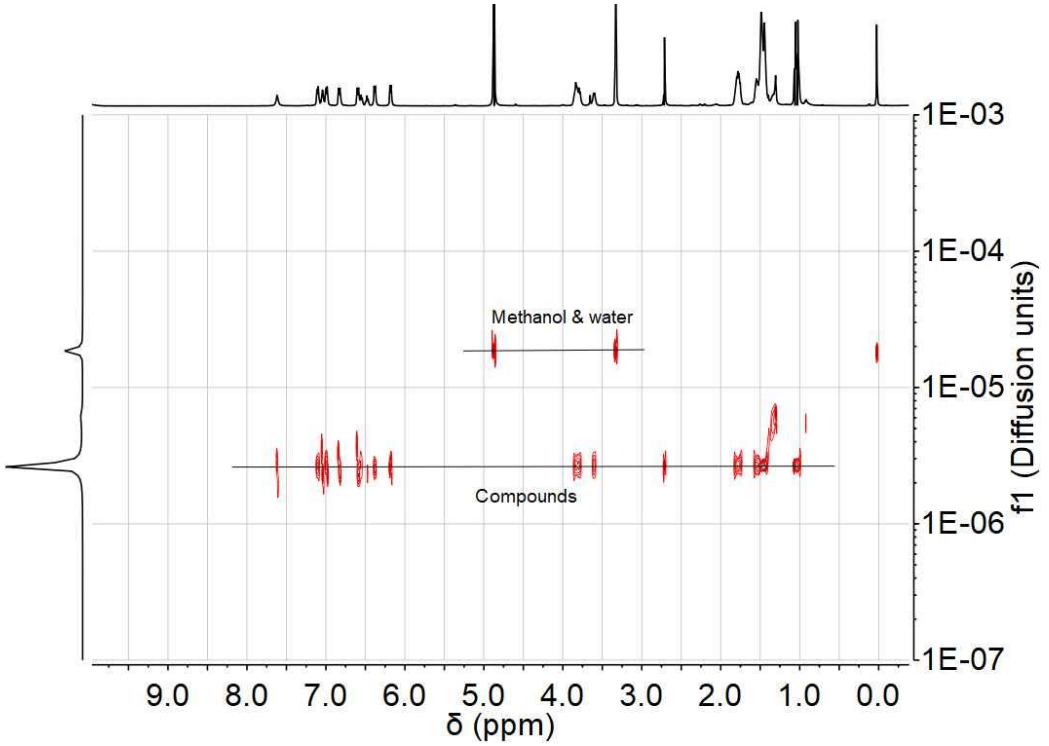


**Figure S28** DOSY spectra (500 MHz, 298 K) of the cationic diPt complex [**2**-$Pt_2$]$^+BF_4^-$ in $CD_3OD$.

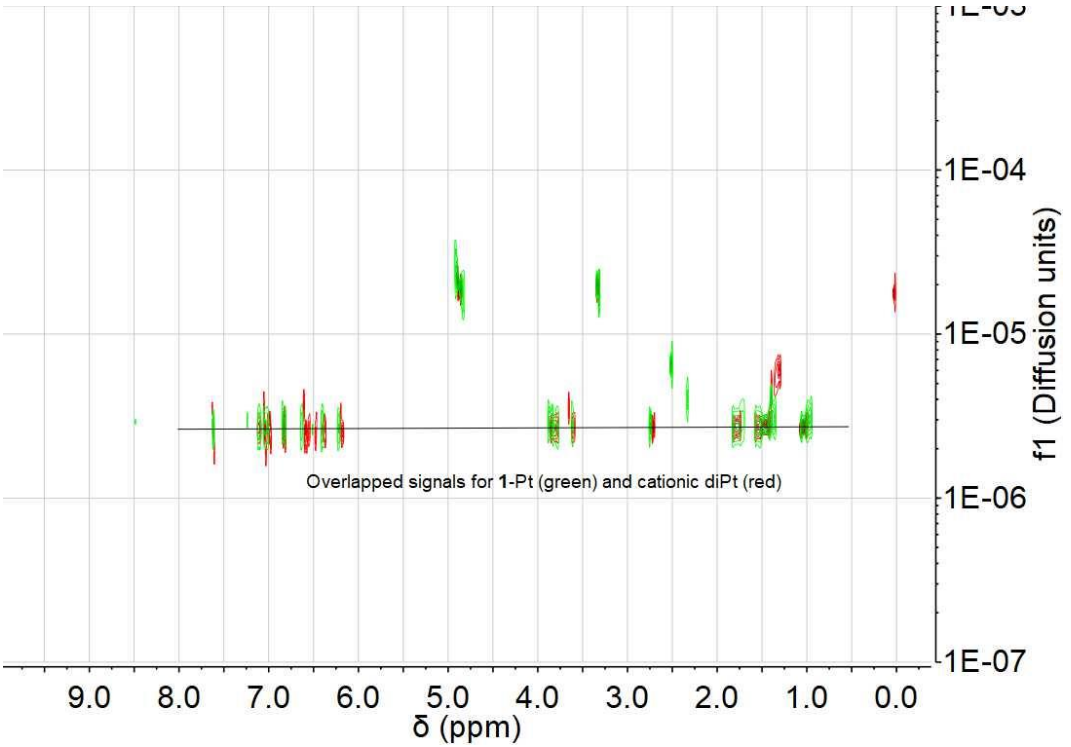


**Figure S29** Overlayed DOSY spectra (500 MHz, 298 K) of **1**-Pt and the cationic diPt complex [**2**-$Pt_2$]$^+BF_4^-$ in $CD_3OD$. The signals of [**2**-$Pt_2$]$^+BF_4^-$ (red) were overlapped with partial signals of **1**-Pt (green), suggesting [**2**-$Pt_2$]$^+$ complex was present in the solution of **1**-Pt in methanol.

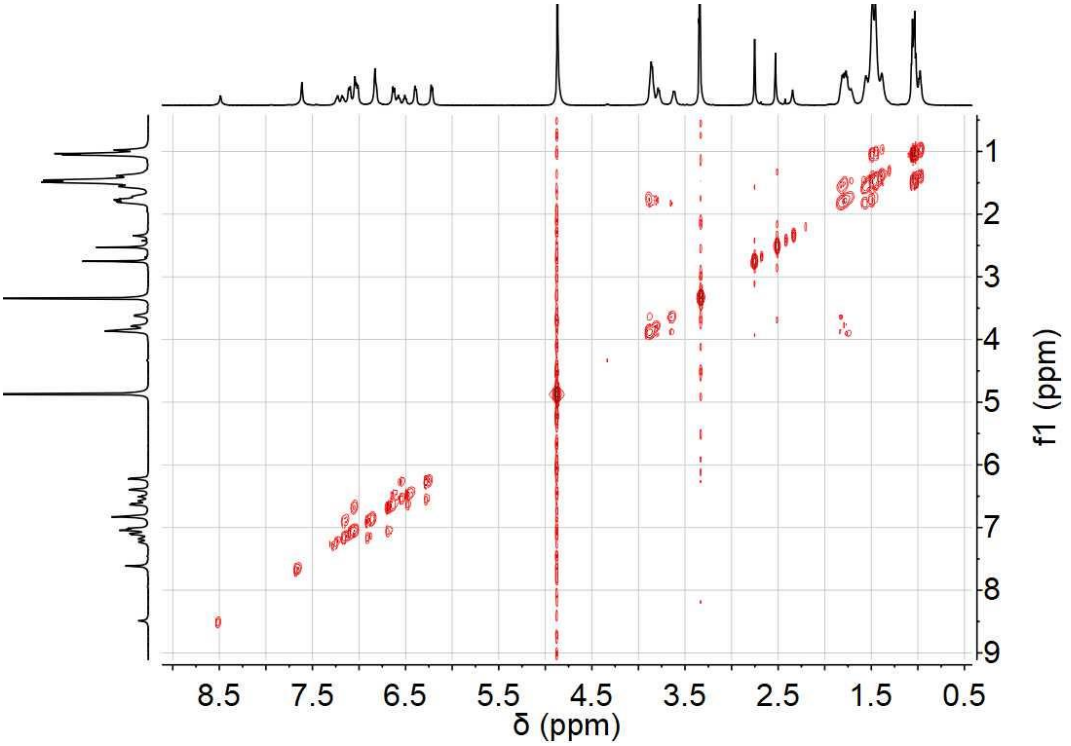


**Figure S30** COSY spectra of **1**-Pt in methanol-$d_4$.

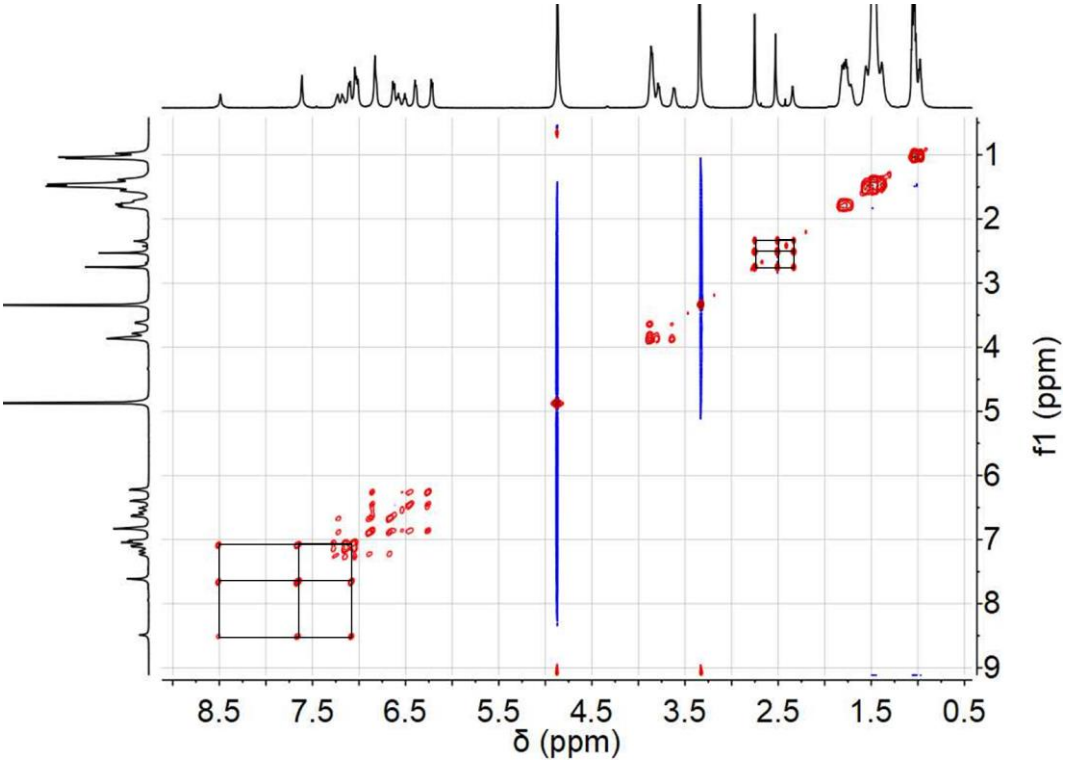


**Figure S31** NOESY spectra of **1**-Pt in methanol-$d_4$.

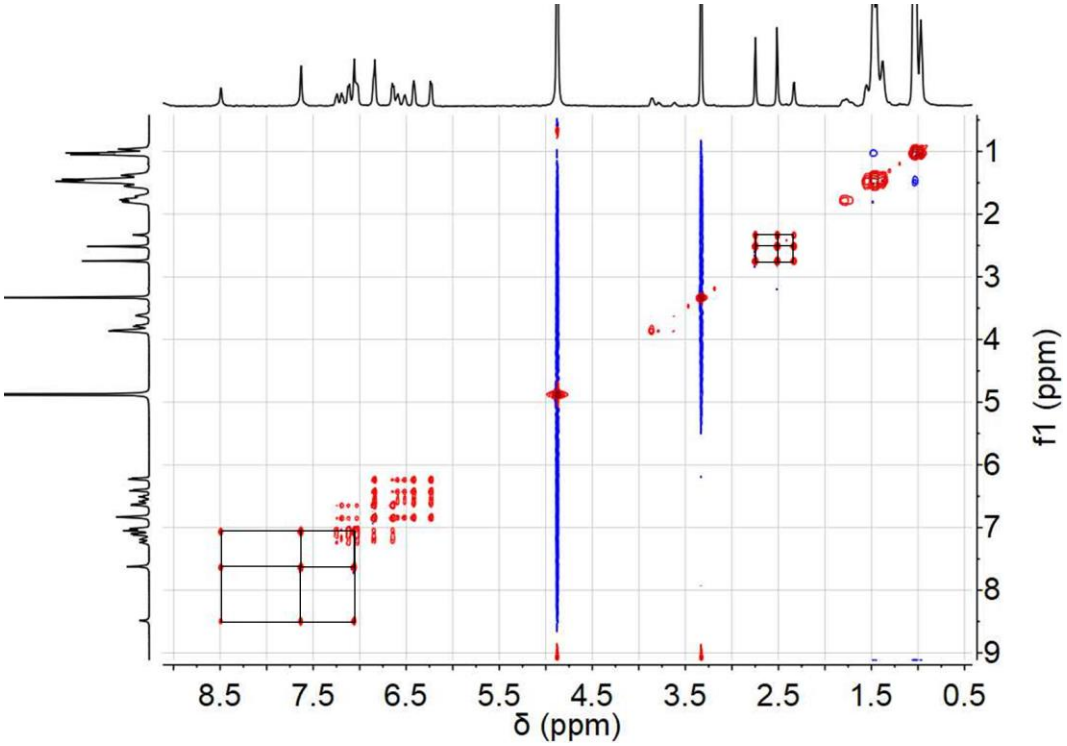


**Figure S32** $^{1}H$-$^{1}H$ EXSY spectra of **1**-Pt in methanol-$d_4$ (298 K, $t_{mix}$ = 2s).

## S4.4 ESI mass spectrometry

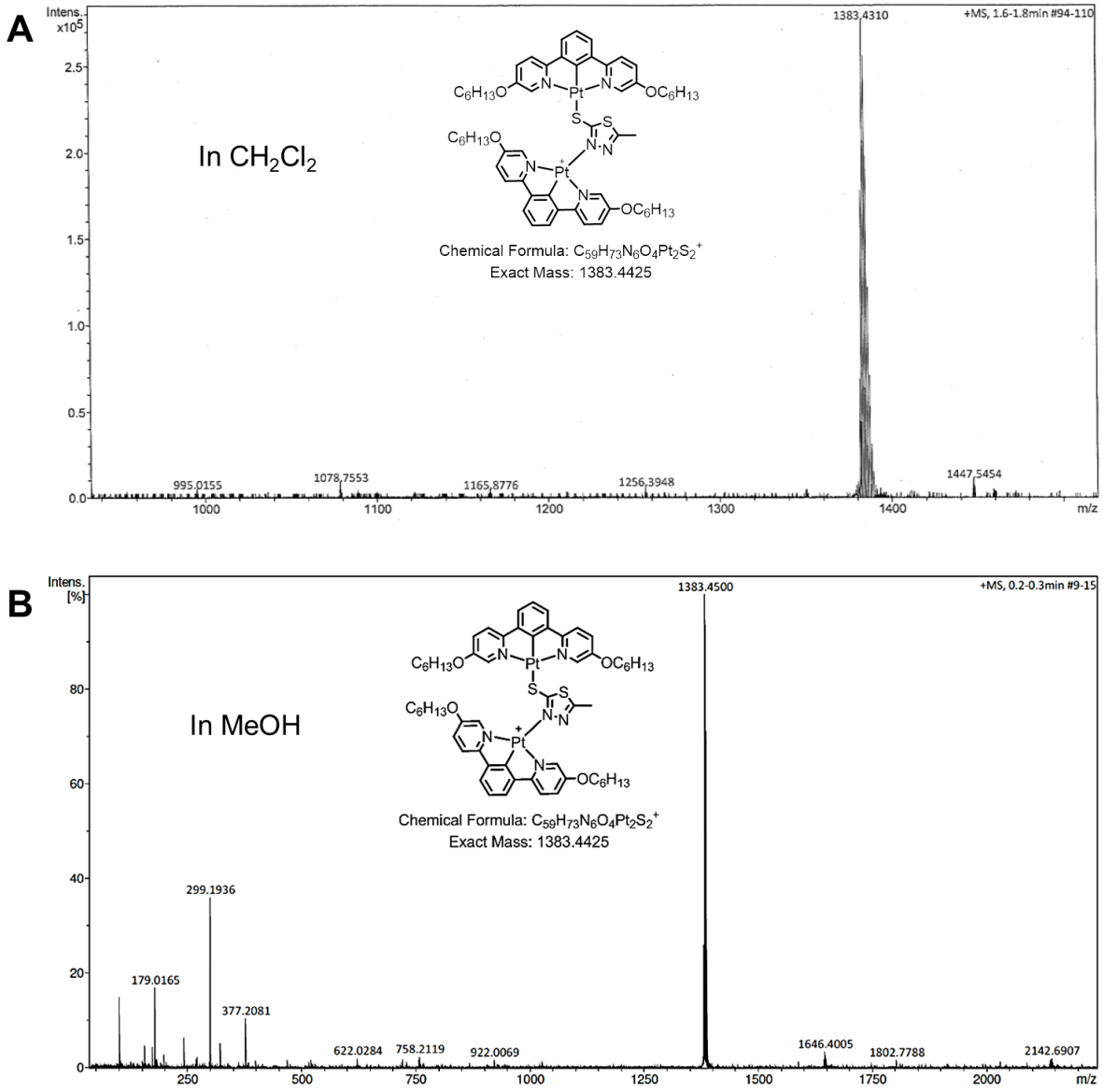


**Figure S33** Electrospray ionisation mass spectrometry of complex **1**-Pt from (**A**) a solution in $CH_2Cl_2$ and (**B**) a solution in MeOH.

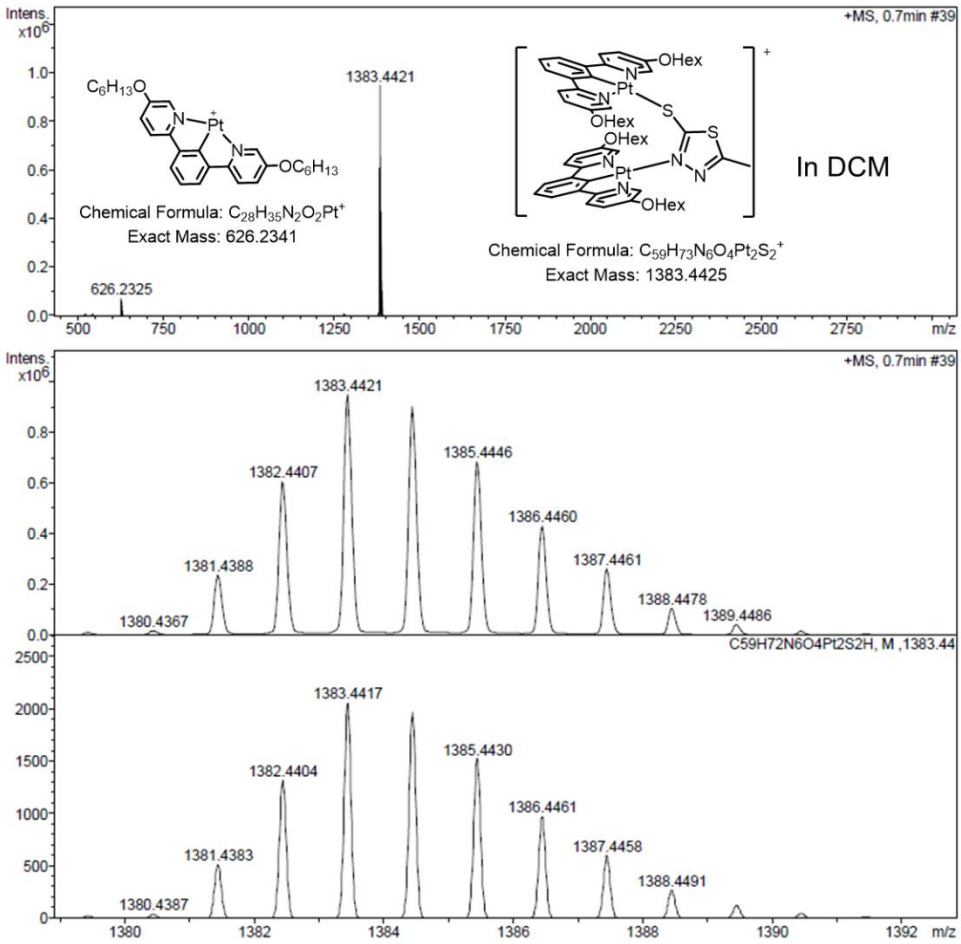


**Figure S34** High resolution electrospray ionisation mass spectrometry of the independently synthesised cationic [**2**-$Pt_2$]$^+BF_4^-$ complex from a solution in $CH_2Cl_2$.

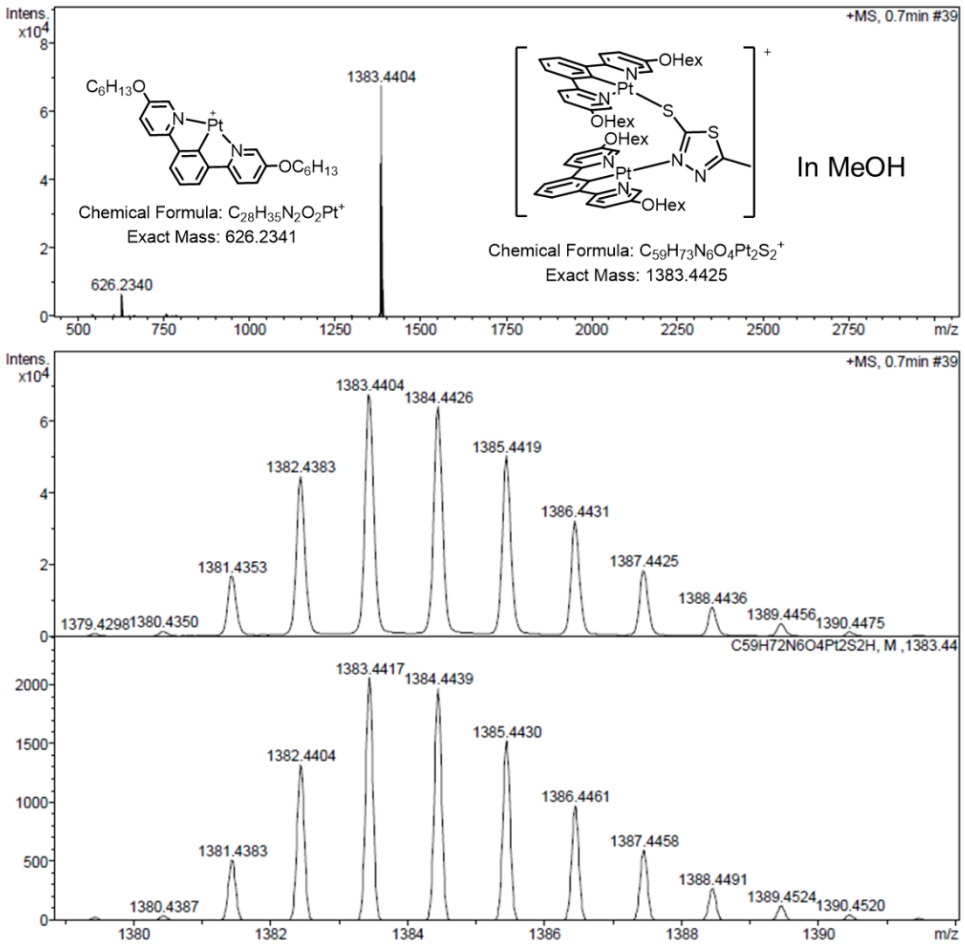


**Figure S35** High resolution electrospray ionisation mass spectrometry of the independently synthesised cationic [**2**-$Pt_2$]$^+BF_4^-$ complex from a solution in MeOH.

### S4.5 Species of 1-Pt in MeOH solution

The $^{1}H$ and $^{195}Pt$ NMR spectra of 1-Pt in methanol-$d_4$ show three distinct groups of peaks, suggesting there are three different chemical environments for Pt centre and some protons.

The independently synthesised cationic [**2**-$Pt_2$]$^{+}BF_4^{-}$ complex displays overlapped peaks with those of **1**-Pt in methanol-$d_4$ (Figure S22), suggesting **1**-Pt in methanol is partially transformed into cationic [**2**-$Pt_2$]$^{+}$ species. Consistent overlapped NMR signals are also observed in the 2D DOSY spectra of **1**-Pt and the cationic [**2**-$Pt_2$]$^{+}$ complex (Figures S26–29). The presence of free thiol ligand (Figure S27), which is detached from **1**-Pt, further confirms the presence of the cationic [**2**-$Pt_2$]$^{+}$ complex. This is further supported by the $^{1}H$-$^{1}H$ NOESY and EXSY spectra (Figures S31-32), in which correlations and exchange are observed for the three $CH_3$ (from the thiol ligand) protons.

# S5. References


[S1] Q. Zheng, S. Borsley, G. S. Nichol, F. Duarte and S. L. Cockroft, *Angew. Chem. Int. Ed.*, 2019, **58**, 12617.

[S2] V. V. Sivchik, E. V. Grachova, A. S. Melnikov, S. N. Smirnov, A. Yu. Ivanov, P. Hirva, S. P. Tunik, and I. O. Koshevoy, *Inorg. Chem.*, 2016, **55**, 3351−3363.